On the Simulated Interplay of External Friction and Thermo-Fluid Dynamics of Glas-Fibre-additivated Polymeric Melt in the Backflow Barrier of a Screw Extruder

D. Trauner, B. Scheichl, H. Schoosleitner*

Kurzfassung

Die Strömung einer mit Glasfasern verstärkten Polymerschmelze durch einen dünnen Spalt, gebildet durch den Sperrring und die Schneckenspitze einer Rückstromsperre eines Schneckenextruders, sowie das damit gekoppelte Wärmeübertragungsproblem werden theoretisch und numerisch behandelt. Unter Anwendung von Dimensionsanalyse wird eine Vielzahl an auftretender Längen- und Zeitskalen betrachtet. Die Strömung wird durch die Schmiertheorie beschrieben. Die rheologisch bedingte volle Kopplung von Impuls- und Wärmetransport wird durch das stark von Scherraten und Temperaturen abhängige Konstitutivgesetz (Ostwald-de-Waele mit Newton'scher Sättigung) beschrieben. Weitere Kopplungseffekte, die von den Scherkräften und der Winkelgeschwindigkeit des Sperrrings und letztlich der (hydrodynamischen bis Misch-)Reibung zwischen diesen beiden Teilen herrühren, bewirken letztlich den wesentlichen Energiefluss in das System. Die eingeführte Modellierung der Mischreibung definiert das Aufliegen des Sperrrings sowie den Ausklinkpunkt in Abhängigkeit des Durchmessers und der Länge der Glasfasern. Verschiedene Phasen des zeitabhängigen Verhaltens bis zum Erreichen eines quasi-stationären Zustandes unter Beachtung der auftretenden Zeitskalen werden präsentiert. Die iterative numerische Lösung des vollständig gekoppelten Problems ermöglicht, unter anderem, die Berechnung der stationären Winkelgeschwindigkeit des Sperrrings. Für gegebene Geometriedaten wird der Arbeitspunkt der Rückstromsperre, gekennzeichnet durch minimale Reibung, abgeleitet.

Schlüsselwörter

Rückstromsperre, Glasfasern, Schmiertheorie, Multiple-Scales-Methode, Ostwald-de-Waele-Fluid, Polymerschmelze, Schneckenextruder

Abstract

The flow of the glass-fibers-carrying polymer melt in the thin gap formed by the locking ring in the backflow barrier of a screw extruder and the associated heat transfer problem are studied theoretically/numerically. Due to the involvement of a multitude of time and length scales, our rigorous approach resorts to the application of dimensional analysis. Though the flow is typically described by lubrication theory, intricacies arise given the rheologically-induced two-sided coupling of the momentum and the thermal-energy transfer via the melts strongly shear-rate- and temperature-dependent non-Newtonian constitutive law (Ostwald-de-Waele fluid exhibiting Newtonian saturation). On the other hand, coupling of the shear forces driving the ring and its spin accounts for essential energy input due to (hydrodynamic to mixed) friction between the ring and the tip of the screw. A model of mixed friction is introduced, using the characteristic diameter and length of glass fibers to define the onset of the ring and the release point. We present different stages of the transient behaviour until steady state given the disparate time scales involved. The iterative numerical solution of the full coupled problem allows for, amongst others, predicting the terminal speed of the locking ring, as a central goal of this study. For a prescribed barrier geometry, the working point exhibiting minimal friction between the locking ring and the tip of screw is derived. This result is potentially of interest in improvements of the barrier design.

Keywords

Backflow barrier, Glass fibres, Lubrication theory, Multiple scaling, Ostwald-de-Waele fluid, Polymer melt, Screw extruder

* Dipl.-Ing. Daniel Trauner, Technische Universität Wien, The Centre for Water Resource Systems, 1040 Vienna
Priv.-Doz. Dipl.-Ing. Dr. Bernhard Scheichl, Technische Universität Wien,
Institute of Fluid Mechanics and Heat Transfer, 1060 Vienna
Dipl.-Ing. Herbert Schoosleitner, Siemens Mobility GmbH, 1110 Vienna

1 Functionality of Barrier and Motivation

Let us consider the widespread extrusion of polymeric melts fortified with glass fibres. The work cycle of the screw extruder can roughly be separated into two phases:

1. **Injection phase** (**figure 1**, bottom): the locking ring (2) lies flat on the stop ring (6), preventing polymeric melt from flowing upstream (5) through the inner gap (1), while weak leakage through the outer gap (3) between locking ring and cylinder wall is possible due to high injection pressure. The whole system, here and in the following consisting of the screw (7), locking ring (2) and stop ring (6), as well as the aforementioned separated gaps, moves in the downstream (8) direction and, with the barrier closed, injects melt into a cavity. During this process, the so-called friction gaps (4) between downstream face of the locking ring and the wings attain their maximum possible height.

2. **Feeding phase** (**figure 1**, top): The screw starts rotating, resulting in rising pressure upstream of the locking ring, thereby pushing the barrier open. This reduces the height of the friction gap and causes the locking ring to almost lie flat on the wings of the screw leading to acceleration of the locking ring about its axis due to friction moments. The motion of the locking ring reaches a steady state, in which its relative angular velocity, with respect to the angular velocity of the screw, is non-zero. Depending on system parameters, hydrodynamic lubrication occurs and is maintained in a steady state in the friction gaps.

   With the locking ring lying flat on the wings of the screw, polymeric melt flows through the system and accumulates downstream of the barrier and forces the whole system of screw and backflow barrier to move in upstream direction. Once enough material for injection has been accumulated, the feeding phase ends and material is injected.

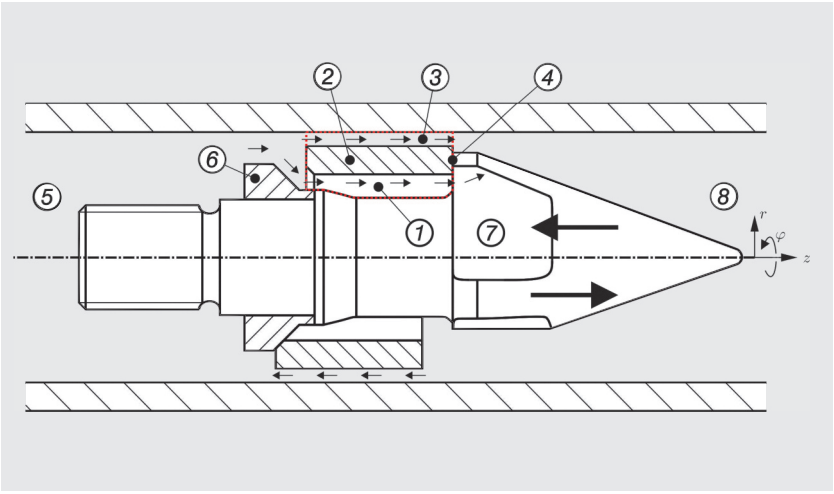

Figure 1: *Backflow barrier and screw tip*

It is the ultimate goal of our study to assess the sensitivity of the dynamical behaviour of the system against material properties during the feeding phase.

2 Statement of the Problem

The task at hand is the calculation of the flow and temperature field in the backflow barrier of a screw extruder. Our study extends and refines previous investigations in a rigorous manner, cf. [1]. We are therefore concerned with the solution to the simplified equations governing mass and heat transfer through the slender and axisymmetric lubrication gaps as well as the locking ring [2, 3]. Under the conventional assumptions, the flow field in the lubrication gaps adheres to the lubrication limit of the full equations of fluid motion:

$$\partial_z p = \rho \partial_n \tau_{nz}, 0 = \partial_\varphi \tau_{n\varphi} \tag{1}$$

Wherein p, ρ, n, z, φ, τ_{nz}, and $\tau_{n\varphi}$ denote respectively pressure, the density, the gap normal direction, the axial direction, the circumferential angle (see **figure 1**), and the associated components of the stress tensor $\boldsymbol{\tau}$ referring to the melt.

The temperature field is the solution to the thermal-energy equation adopted in full so as to account for weak geometric curvature effects:

$$\rho c_p D_t T = \lambda \nabla^2 T + \dot{\phi}. \tag{2}$$

Herein c_p, T, λ and $\dot{\phi}$ are the specific heat capacity, the temperature, the thermal conductivity, and the dissipation function, respectively. Accordingly, the temperature in the locking ring is described by the heat conduction equation

$$\rho c_p \partial_t T = \lambda \nabla^2 T. \tag{3}$$

The polymeric melt flowing through the backflow barrier exhibits a non-Newtonian constitutive law. It is preferably modelled as an Ostwald-de Waele (power-law) fluid [4, 5]:

$$\eta = k a_T \|\dot{\boldsymbol{\gamma}}\|^{m-1}, \boldsymbol{\tau} = \eta(\dot{\boldsymbol{\gamma}}, T)\dot{\boldsymbol{\gamma}} \tag{4}$$

Wherein k is the power-law consistency index, $m > 0$ the flow-behavior index, and the correction a_T takes the temperature dependency by virtue of the Arrhenius-Ansatz into account. Most important, the scalar viscosity is a function of the flow field by means of $\dot{\boldsymbol{\gamma}}$, i. e. twice the rate-of-strain tensor.

3 Modelling of Mixed Friction

The wings of the extruder screw are bevelled at the leading edge (in relation to its velocity), trying to achieve hydrodynamic lubrication in the friction gap, to reduce wear. The flow in the friction gap is described by equation (1), which is an equation of continuum mechanics and does not take glass fibres in the polymeric melt into account, leading to underestimated friction between the locking ring and the wings. This is corrected by interpolating between a calculated hydrodynamic and an experimental coefficient of friction, as can be seen in **figure 2**.

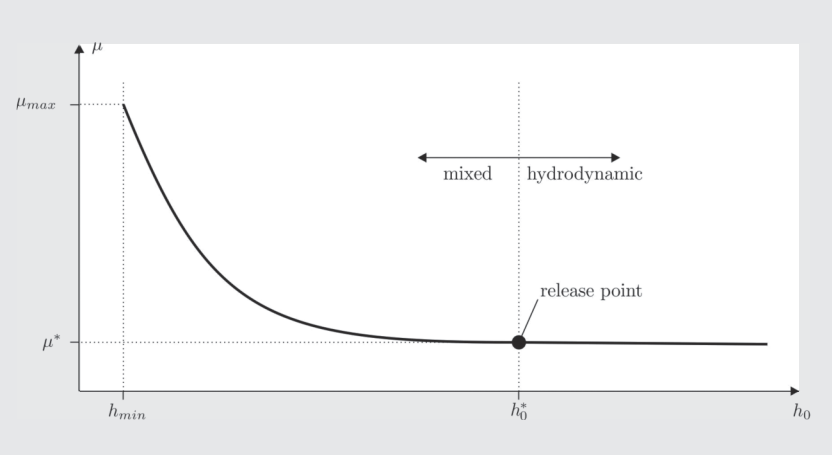

Figure 2: *Modelling of coefficient of friction*

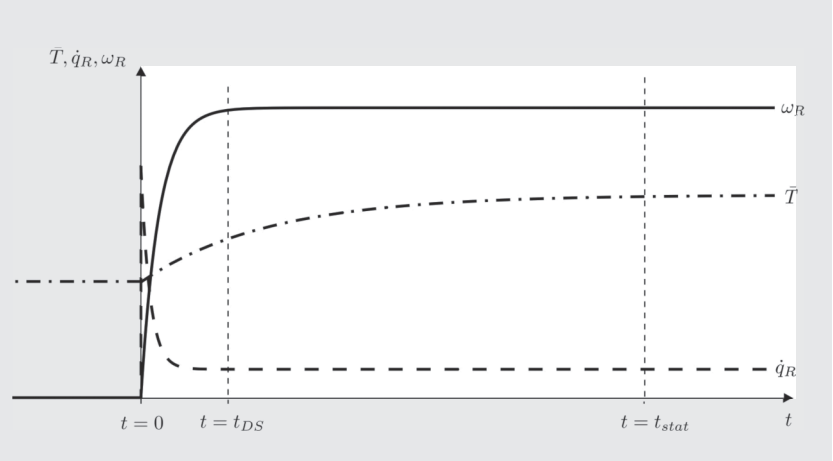

Figure 3*: Characteristic times and scale separation*

4 Scale Separation

Out of the different physical effects in the system, a multitude of characteristic time scales arises. At first, the time needed to open the backflow barrier initializing the feeding phase, estimated by inspection of Newton's second law, is much smaller than the time scales entering the heat and thermal-energy equations as these depend on length scales representative of the system and the thermal diffusivities of the ring and the melt. Secondly, the time scale describing the acceleration of the locking ring estimated by the principle of angular momentum is comparatively smaller than the time scales introduced by the thermal-energy equations.

A first result of this inspection analysis is the splitting of the feeding phase as shown in **figure 3**: the characteristic values of angular velocity ω_R and mean temperature $\overline{T}$ of the ring as well of the friction heat flux $\dot{q}_R$ into the ring are depicted over time. Hence, the processes of opening the backflow barrier and accelerating the locking ring have an insignificant impact on the resulting flow and temperature field, given their small time-scales. Therefore, these effects are neglected, the calculations start at $t = t_{DS}$, denoting the time representative for the acceleration of the ring, where the flow has already attained a fully developed state but thermal diffusion and dissipation have not, until $t = t_{stat}$ $(t_{stat}/t_{DS} \gg 1)$.

5 Numerical Simulation and Results

The equations stated in section 2 are solved by applying finite-difference approximations. The different domains of locking ring and inner, outer and friction gap are fully coupled, considering both motion and temperature. Nonlinearities, introduced by the constitutive law of the polymeric melt, necessitate an iterative solution involving a hierarchy of iteration loops.

A robust algorithm was developed, consisting of three iteration loops for calculation of motion and temperature, the minimal friction gap width and the steady angular velocity of the ring, respectively. Boundary conditions for these calculations are the angular velocity of the screw, the pressure difference between in- and outflow and the temperature of the screw and the wall.

5.1 Flow and Temperature Fields

The following results are calculated using an optimal inclination angle of the wings, which is derived in section 5.3, and can be seen in **figure 5**.

As shown in **figure 4**, the velocity of the polymer melt along the axial direction reaches its maximum at the narrowest point of the inner gap. Corresponding to the shear-thinning effect, zones of high shear rates show low viscosity and vice versa. Due to the relative rotational

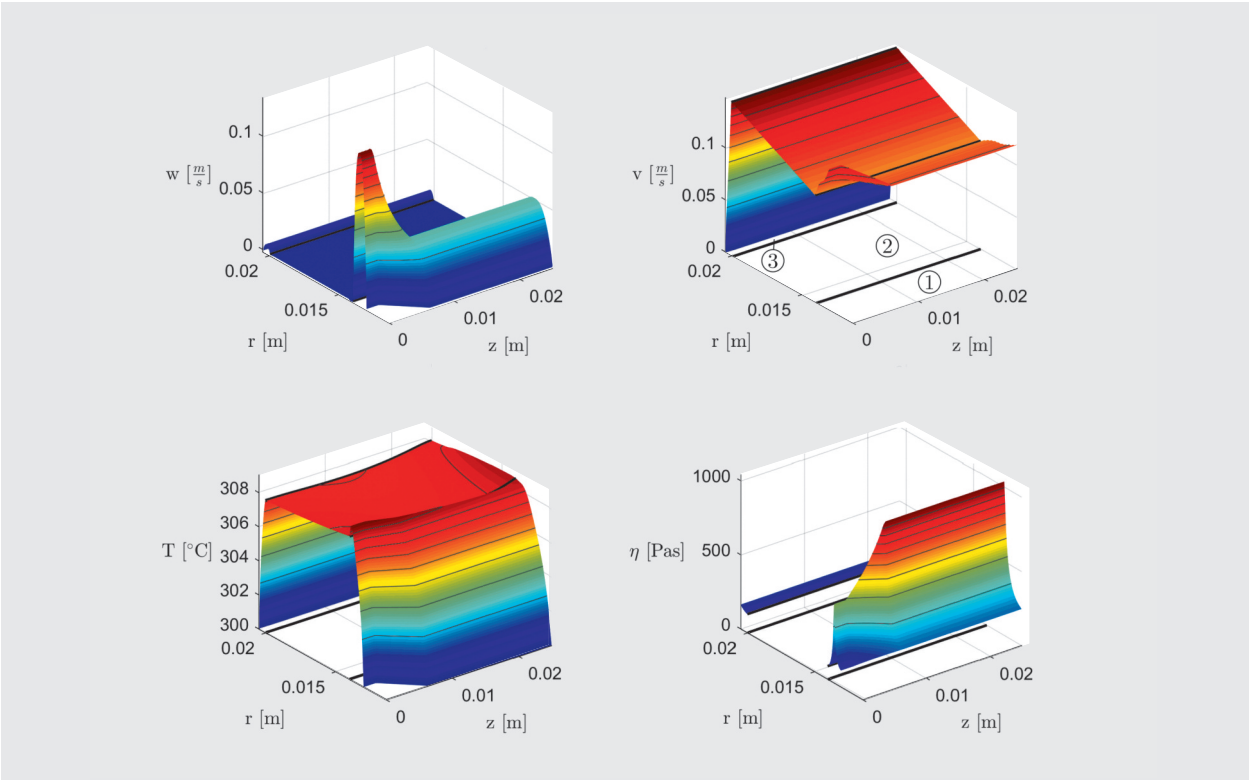

Figure 4: *Surface plots of axial velocity (top left), azimuthal velocity (top right), temperature (bottom left) and viscosity (bottom right); (1) inner gap, (2) locking ring, (3) outer gap*

velocity of the ring, the occurrence of vanishing shear rates is prevented, which otherwise would lead to indefinite viscosity. The effect of the shear rate on the dissipation function can be observed in the bottom left plot of **figure 4**, where higher temperature in the melt relates to high dissipation. The reason for the slightly increased temperature at the ring's downstream face is friction with the wings of the screw tip.

5.2 Comparison with Strictly Newtonian Case

Figure 5 shows the pressure distribution of a Newtonian and non-Newtonian fluid along the unwound span φ^* of a single wing as well as its geometry. The Newtonian solution serves as a validation of the numerical approach, considering that the power-law coefficient in this case is $m = 1$. The smaller this coefficient, i. e. the more shear-thinning the fluid, the farther the peak of the pressure curve shifts to the narrowest part of the gap (to the left in **figure 5**).

The viscosity for the Newtonian reference case is defined as the so-called representative viscosity [2], which is found by demanding equal volume flux through the backflow barrier considering Newtonian and non-Newtonian flow.

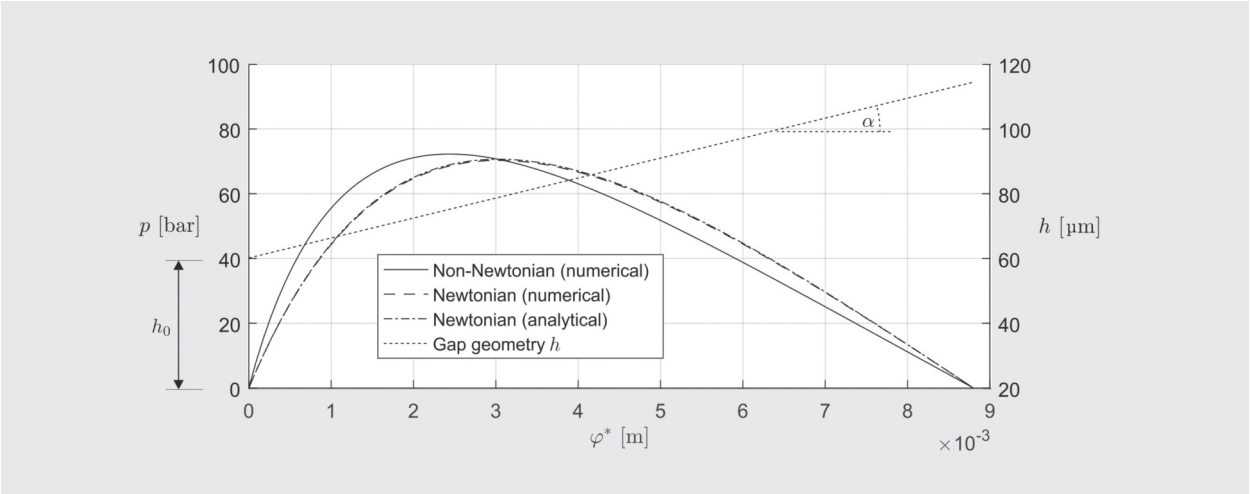

Figure 5: *Pressure distribution in friction gap; difference between Newtonian and non-Newtonian melt*

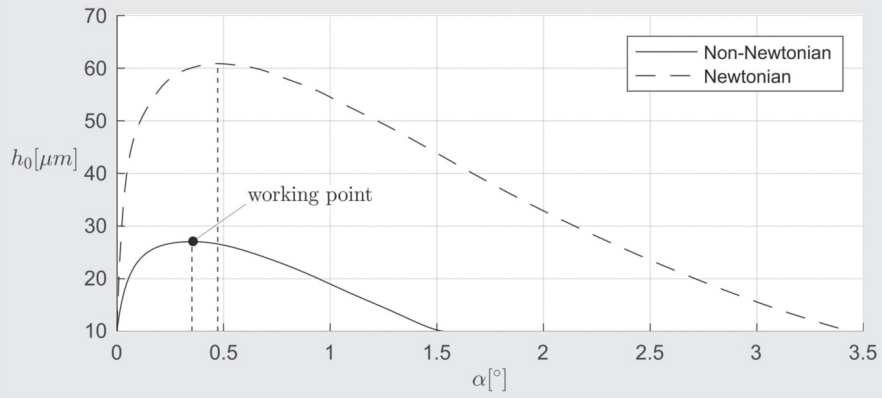

Figure 6: *Influence of inclination angle on minimal width of friction gap*

5.3 Influence of Inclination Angle

The gap width between the wings and the locking ring has a determining influence on both motion and temperature. Therefore, the goal is to determine the optimal inclination angle of the face of the wing (see **figure 5**) maximizing the gap width to reduce or even prevent mixed friction. As seen in **figure 6**, the optimum angle for Newtonian fluids yields $\alpha = 0.4°$, for non-Newtonian fluids the most advantageous angle is $\alpha = 0.32°$.

The minimum value for h_0 is determined by the mean diameter of the glass fibers, relating to the modelling of mixed friction in section 3. The working point in **figure 6** represents the maximal gap width in the feeding phase correlating with minimal wear.

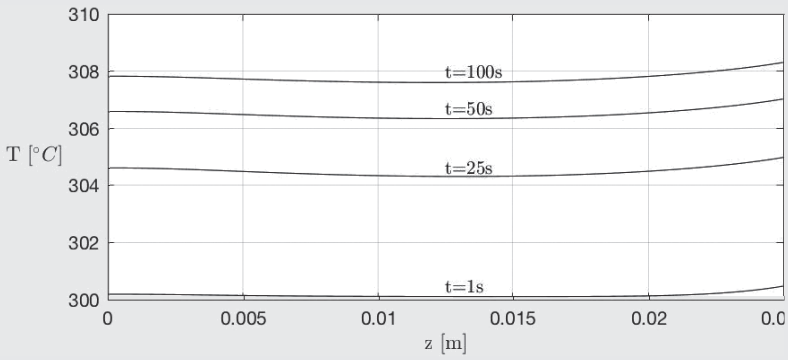

Figure 7: *Evolution of temperature along the midsurface of the ring (r = 17 mm); inlet face isolated (left), outlet face exposed to friction heat (right)*

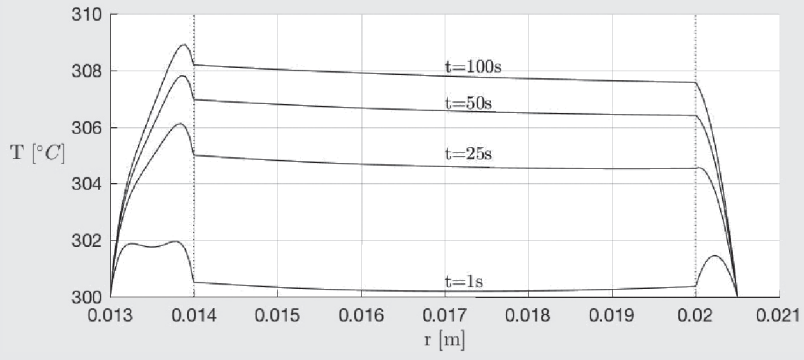

Figure 8: *Evolution of temperature in radial direction at the inlet (z = 0 mm)*

5.4 Transient Heat Conduction

As described in section 4, flow and motion of the locking ring reach their steady state before heat is distributed to an equilibrium. This allows the assumption of constant dissipation and friction power, while the time-dependent temperature field is calculated starting at a uniform distribution of temperature. **Figure 7** and **8** show temperature evolutions along axial and radial directions, respectively.

6 Concluding remarks

By resorting to the first principles and their rational simplification, we have substantially reduced the complexity associated with the dynamics of the locking ring of a backflow barrier and advanced in understanding its dependence on external frictional power and internal frictional losses. The latter is intrinsically tied in with the heat transport across the ring, as a consequence of the highly non-Newtonian rheology of the polymer melt, fortified with glass fi-

bres. Chances are high that the first systematic numerical simulations pave the way for further improvements regarding the barrier design, e. g. so as to control the ring dynamics. Future efforts comprise, amongst others, a higher-order time-stepping for coping reliably with the quite disparate time scales involved in fully transient calculations. By reappraising the analytical aspects of the problem parallel to the numerical simulations, deeper insight is expected to ensue from completing the indicated rigorous multiple time-scales analysis.

Acknowledgements

Financial support of the Austrian Research Promotion Agency (FFG) within the COMET K2 program (grant no.: 849109, project acronym: *XTribology*) is gratefully acknowledged.

References

[1] C.J. GORNIK: Neue Erkenntnisse zur Plastifiziereinheit von Spritzgießmaschinen basierend auf experimentellen Untersuchungen. Dissertation, Monatnuniversität Leoben, 2007.

[2] H. SCHLICHTING, and K. GERSTEN: Boundary Layer Theory, 9th edition. Springer Berlin, Heidelberg, 2017.

[3] F. DURST: Fluid Mechanics (An Introduction to the Theory of Fluid Flows). Springer Berlin, Heidelberg, 2007.

[4] G. MENGES, E. HABERSTROH, W. MICHAELI and E. SCHMACHTENBERG: Menges Werkstoffkunde Kunststoffe. Carl Hanser Verlag, München. 2011.

[5] A.K. TOWNSEND and H.J. WILSON: The fluid dynamics of the chocolate fountain. European Journal of Physics, Vol 37(1), p.015803 (24p), 2016.